

A RIS-Based Passive DOA Estimation Method for Integrated Sensing and Communication System

Zhimin Chen, *Member, IEEE*, Peng Chen, *Member, IEEE*, Ziyu Guo, *Member, IEEE*,
Xianbin Wang, *Fellow, IEEE*

Abstract—Integrated sensing and communication (ISAC) system has received growing attention, especially in the context of B5G/6G development. Combining the reconfigurable intelligent surface (RIS) with wireless communication process, a novel passive sensing technique is formulated in this paper to estimate the direction of arrival (DOA) of the targets, where the control matrix of the RIS is used to realize the multiple measurements with only one full-functional receiving channel. Unlike the existing methods, the interference signals introduced by wireless communication are also considered. To improve the DOA estimation, a novel atomic norm-based method is proposed to remove the interference signals by the sparse reconstruction. The DOA is estimated after the interference removal by a novel Hankel-based multiple signal classification (MUSIC) method. Then, an optimization method is also developed for the measurement matrix to reduce the power interference signals and keep the measurement matrix's randomness, which guarantees the performance of the sparse reconstruction. Finally, we derive the theoretical Cramér-Rao lower bound (CRLB) for the proposed system on the DOA estimation. Simulation results show that the proposed method outperforms the existing methods in the DOA estimation and shows the corresponding CRLB with different distributions of the sensing node. The code about the proposed method is available online <https://github.com/chenpengseu/PassiveDOA-ISAC-RIS.git>.

Index Terms—atomic norm minimization, DOA estimation, Integrated sensing and communication, passive sensing method, reconfigurable intelligent surface.

I. INTRODUCTION

INTEGRATED sensing and communication (ISAC) [1] system has attracted growing attentions in recent years due to its potential of meeting diverse needs of location-based applications. The principle of ISAC is similar to the joint communication and radar sensing (JCR) system [2],

This work was supported in part by the Natural Science Foundation of Shanghai (Grant No.22ZR1425200), the Equipment Pre-Research Field Foundation, the Industry-University-Research Cooperation Foundation of The Eighth Research Institute of China Aerospace Science and Technology Corporation (Grant No. SAST2021-039), the National Key R&D Program of China (Grant No. 2019YFE0120700), the National Natural Science Foundation of China (Grant No. 61801112), and the Natural Science Foundation of Jiangsu Province (Grant No. BK20180357). (Corresponding author: Peng Chen)

Z. Chen is with the School of Electronic and Information, Shanghai Dianji University, Shanghai 201306, China, and also with the Department of Electronic and Information Engineering, The Hong Kong Polytechnic University, Hong Kong (e-mail: chenzm@sdju.edu.cn).

P. Chen is with the State Key Laboratory of Millimeter Waves, Southeast University, Nanjing 210096, China (e-mail: chenpengseu@seu.edu.cn).

Z. Guo is with the State Key Laboratory of ASIC and System, Fudan University, Shanghai 201203, China (email: zguo@fudan.edu.cn).

X. Wang is with the Department of Electrical and Computer Engineering, Western University, London, ON N6A 5B9, Canada (e-mail: xianbin.wang@uwo.ca).

where both the target sensing and wireless communication functions are concurrently realized [3]–[6]. In an ISAC system, a target can be sensed either in an active way with dedicated signal transmitted for sensing [7], or in a passive way, where the estimation of the parameters including the velocity and position is achieved based on the reception of other signals unrelated to sensing (e.g. communication signals). In [8], an overview of the modulation schemes for JCR is given for the joint sensing and communication performance, and a comparative analysis is also carried out. Similar to the radar system, device-free sensing is that we use the reflected communication signal to sense a target, and the device-free sensing method for moving target using orthogonal frequency division multiplexing (OFDM) is developed in [9].

A sensor can be easily added to an existing wireless communication system for preliminary passive sensing. For example, a WiFi-based sensing method is proposed in [10] to estimate human activity nearby. In [11], target localization with the one-bit analog-to-digital-converter (ADC) is proposed for the internet-of-things application. For the device-free localization, authors of [12] used the phase response shift to localize targets and improve the localization performance. Recently, reconfigurable intelligent surface (RIS) has been adopted in wireless communication for controlled reconfiguration of communication environment [13,14]. With this development, the RIS-based localization methods have also been exploited recently. In [15], a near-field localization method is addressed using compressed sensing (CS), and authors of [16] proposed a JCR system with RIS.

In the passive sensing system, the sensor receives conventional communication signals for target localization based on the direction-finding or the direction of arrival (DOA) estimation. However, the resolution of traditional DOA estimation using the fast Fourier transformation (FFT) is limited. To improve the DOA estimation accuracy while keep complexity low, super-resolution methods based on subspace have been proposed, such as the multiple signal classification (MUSIC) algorithm [17], and estimation of signal parameters via rotational invariance techniques (ESPRIT) [18]. With the development of compressed sensing (CS), sparse reconstruction methods have also been proposed for the DOA estimation [19]–[21]. In most CS-based methods, the spatial domain is discretized into grids, which will introduce the *off-grid* error since the targets cannot be at the grids exactly [22,23]. The continuous domain methods based on the sparse reconstruction have been further proposed to overcome this error. For example, an atomic norm minimization (ANM) is proposed for the

DOA estimation in [24]–[26], where an atomic set is defined. In [27], a single snapshot super-resolution method is proposed for the DOA estimation in arbitrary array geometries. A fractional Fourier transform-based method is proposed in [28] by combining the ANM. Ref. [29] shows an ANM-based method using irregular Vandermonde decomposition.

In this paper, we formulate a passive sensing system based on DOA estimation. The RIS is used to realize the multiple measurements, and a sensor with only one full-functional receiving channel estimates the DOA of targets. Different from the existing sensing methods, we consider a passive sensing method, where the receiving signals are interfered by unwanted signals. Then, a novel atomic norm-based method is proposed for the interference removal, and the DOA is estimated by a novel Hankel-based MUSIC method. Moreover, the measurement matrix is also optimized to improve the DOA estimation performance and break the error platform in the DOA estimation method. Finally, the theoretical Cramér–Rao lower bound (CRLB) for the proposed system model is derived. The contributions of this paper are listed as follows:

- **A passive sensing system** is proposed using RIS, where only one full-channel receiving is adopted, and the interference signals in the proposed system are well described.
- **A novel DOA estimation method** is proposed based on the atomic norm, where the sparse Reconstruction removes the interference signal. Then, a Hankel-based MUSIC method is proposed for the spatial spectrum estimation with only less number of the RIS measurements.
- **A novel optimizing method for measurement matrix** is formulated to control the RIS by removing the interference signal and breaking the error platform of the DOA estimation. A random vector is introduced to ensure the randomness of RIS measurement.
- **The CRLB for the DOA estimation** is obtained for the proposed passive sensing system, which can optimize the system, such as the locations of the wireless access point (AP), the RIS, and the sensor.

The remainder of this paper is organized as follows. The RIS system model for passive DOA estimation is given in Section II. The proposed DOA estimation method is proposed in Section III. Then, the measurement matrix is optimized by the proposed in Section IV. Simulation results are carried out in Section VI, and finally, Section VII concludes the paper.

Notations: Upper-case and lower-case boldface letters denote matrices and column vectors, respectively. The matrix Hermitian and transpose are denoted as $(\cdot)^H$ and $(\cdot)^T$, respectively. $\mathcal{R}\{\cdot\}$ denotes the real part of a complex value, respectively. $\text{Tr}\{\cdot\}$ is the trace of a matrix. $\|\cdot\|_1$ and $\|\cdot\|_2$ are the ℓ_1 and ℓ_2 norms, respectively. $\mathcal{E}(\cdot)$ is the expectation operation. j is defined as $j \triangleq \sqrt{-1}$. \mathbb{C} denotes the set of complex numbers.

II. THE RIS SYSTEM MODEL FOR PASSIVE DOA ESTIMATION

This paper considers a RIS-based sensing system to localize the targets in a scenario using wireless communication signals. As shown in Fig. 1, a wireless AP transmits the wireless

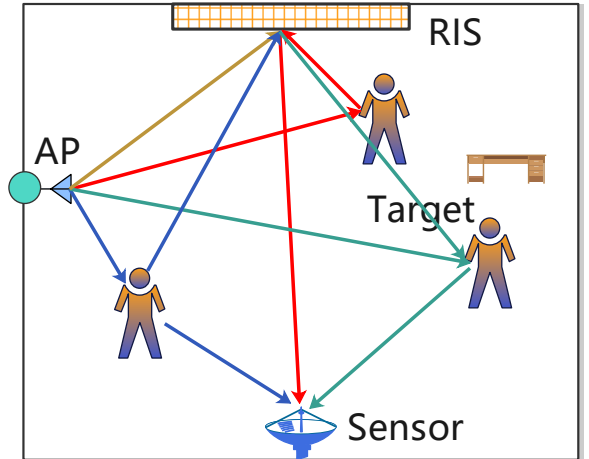


Fig. 1. The passive sensing model using RIS and sensor with one full-functional receiver.

communication signals to the users, and we try to use this type of signal to sense the targets by using a receiving sensor with only one full-functional receiving channel. The RIS is equipped on the wall and can reflect all the received signals, and the transmitted signal in AP is denoted as $s(t)$. This paper considers a two-dimensional (2D) localization and can be easily extended to a three-dimensional (3D) one. Assume that there are K targets, and the position of the k -th ($k = 0, 1, \dots, K-1$) target is denoted as $\mathbf{p}_k = (x_k, y_k)$. The distance between the AP and the k -th target is denoted as $d_{\text{AT},k}$, and the distance between the k -th target and RIS is $d_{\text{TR},k}$.

We consider a RIS with M elements, and assume that the elements form a uniform linear array (ULA) with the distance between adjacent elements being d_E . The DOA between the k -th target and the RIS is denoted as $\theta_{\text{TR},k}$, and the DOA between the AP and the RIS is θ_{AR} . Therefore, the superimposed signal received by the m -th ($m = 0, 1, \dots, M-1$) element in RIS can be expressed as

$$x_m(t) = \sum_{k=0}^{K-1} \frac{\alpha_k}{d_{\text{AT},k} d_{\text{TR},k}} s(t - \tau_{\text{ATR},k}) e^{j \frac{2\pi m d_E}{\lambda} \sin \theta_{\text{TR},k}} + \frac{\beta}{d_{\text{AR}}} s(t - \tau_{\text{AR}}) e^{j \frac{2\pi m d_E}{\lambda} \sin \theta_{\text{AR}}}, \quad (1)$$

where λ is the wavelength, α_k is a constant corresponding to the scattering coefficient of the k -th target, and β is that of the direct path between the AP and RIS. $\tau_{\text{ATR},k}$ denotes the delay of the path from the AP to the k -th target and received by the RIS. We denote the delay from the AP to the RIS as τ_{AR} .

During the n -th ($n = 0, 1, \dots, N-1$) time slot nT , the reflected signal in the m -th ($m = 0, 1, \dots, M-1$) element is

$$y_{m,n}(t) = A_{m,n} e^{j \phi_{m,n}} x_m(t), \quad (2)$$

where $A_{m,n}$ is the reflection amplitude and $\phi_{m,n}$ is the corresponding phase. Considering the direction between the

RIS and sensor is θ_{RS} , the received signal in the sensor with only one full-functional receiving channel can be obtained as

$$\begin{aligned} r_n(t) = & \sum_{m=0}^{M-1} \frac{\gamma}{d_{\text{RS}}} y_{m,n}(t - \tau_{\text{RS}}) e^{j \frac{2\pi m d_{\text{E}}}{\lambda} \sin \theta_{\text{RS}}} + w_n(t) \\ & + \sum_{k=0}^{K-1} \frac{\alpha'_k}{d_{\text{AT},k} d_{\text{TS},k}} s(t - \tau_{\text{ATS},k}) + \frac{\beta'}{d_{\text{AS}}} s(t - \tau_{\text{AS}}) \\ & + \sum_{k=0}^{K-1} \sum_{m=0}^{M-1} \frac{\alpha''_k}{d_{\text{RT},k} d_{\text{TS},k}} y_{m,n}(t - \tau_{\text{RT},k} - \tau_{\text{TS},k}) \\ & e^{j \frac{2\pi m d_{\text{E}}}{\lambda} \sin \theta_{\text{RT},k}}, \end{aligned} \quad (3)$$

where the delay between the RIS and the sensor is τ_{RS} , and $w_n(t)$ is the additive white Gaussian noise (AWGN). The delay τ_{ATS} is that from the AP to the sensor through the target, and the delay τ_{AS} is the direct path from the AP to the sensor. d_{RS} is the distance between the RIS and the sensor. α'_k , β' and γ are the constants for the path and scattering attenuation. Note that the signals reflected by more times have been ignored, since the power is much lower than that of other signals. Additionally, we assume that the size of RIS is much smaller than the bandwidth B of the signal, so the delay between the elements in RIS can be described by the phase factor $e^{j \frac{2\pi m d_{\text{E}}}{\lambda} \sin \theta_{\text{RT},k}}$.

Finally, by ignoring the signal with much lower power, the received signal $r_n(t)$ can be simplified as

$$\begin{aligned} r_n(t) \approx & \sum_{m=0}^{M-1} \sum_{k=0}^{K-1} A_{m,n} e^{j \phi_{m,n}} e^{j \frac{2\pi m d_{\text{E}}}{\lambda} \sin(\theta_{\text{RS}} + \sin \theta_{\text{TR},k})} \\ & \frac{\gamma \alpha_k}{d_{\text{AT},k} d_{\text{TR},k} d_{\text{RS}}} s(t - \tau_{\text{ATRS},k}) \\ & + \sum_{m=0}^{M-1} A_{m,n} e^{j \phi_{m,n}} e^{j \frac{2\pi m d_{\text{E}}}{\lambda} \sin(\theta_{\text{RS}} + \theta_{\text{AR}})} \\ & \frac{\gamma \beta}{d_{\text{AR}} d_{\text{RS}}} s(t - \tau_{\text{ARS}}) + w_n(t) \\ & + \sum_{k=0}^{K-1} \frac{\alpha'_k}{d_{\text{AT},k} d_{\text{TS},k}} s(t - \tau_{\text{ATS},k}) + \frac{\beta'}{d_{\text{AS}}} s(t - \tau_{\text{AS}}) \\ & + \sum_{k=0}^{K-1} \sum_{m=0}^{M-1} \frac{\alpha''_k \beta}{d_{\text{AR}} d_{\text{RT},k} d_{\text{TS},k}} A_{m,n} e^{j \phi_{m,n}} \\ & s(t - \tau_{\text{ARTS},k}) e^{j \frac{2\pi m d_{\text{E}}}{\lambda} (\sin \theta_{\text{RT},k} + \sin \theta_{\text{AR}})} \end{aligned} \quad (4)$$

where we denote the delay $\tau_{\text{ATRS},k} \triangleq \tau_{\text{ATR},k} + \tau_{\text{RS}}$, $\tau_{\text{ARS}} \triangleq \tau_{\text{AR}} + \tau_{\text{RS}}$ and $\tau_{\text{ARTS},k} \triangleq \tau_{\text{AR}} + \tau_{\text{RT},k} + \tau_{\text{TS},k}$.

From the expression of the received signal $r_n(t)$, we can find that the received signal is composed of various signals with different power. To localize the targets and improve the power of interesting signals, we must design the receiving beam of the sensor so that the power in the path from the RIS to the sensor can be improved, and other paths received by the sensor can be ignored. Hence, we have $0 \approx \alpha'_k \approx \alpha''_k \approx \beta' \ll \gamma$. Then, the received signal can be simplified as

$$r_n(t) \approx \sum_{m=0}^{M-1} \sum_{k=0}^{K-1} A_{m,n} e^{j \phi_{m,n}} e^{j \frac{2\pi m d_{\text{E}}}{\lambda} \sin(\theta_{\text{RS}} + \sin \theta_{\text{TR},k})}$$

$$\begin{aligned} & \frac{\gamma \alpha_k}{d_{\text{AT},k} d_{\text{TR},k} d_{\text{RS}}} s(t - \tau_{\text{ATRS},k}) \\ & + \sum_{m=0}^{M-1} A_{m,n} e^{j \phi_{m,n}} e^{j \frac{2\pi m d_{\text{E}}}{\lambda} \sin(\theta_{\text{RS}} + \theta_{\text{AR}})} \\ & \frac{\gamma \beta}{d_{\text{AR}} d_{\text{RS}}} s(t - \tau_{\text{ARS}}) + w_n(t), \end{aligned} \quad (5)$$

where the paths AP \rightarrow targets \rightarrow RIS \rightarrow sensor and AP \rightarrow RIS \rightarrow sensor are kept.

In the RIS-based sensing system, we assume that we can change the reflection coefficient $A_{m,n} e^{j \phi_{m,n}}$ with a frequency $1/T$, which is much faster than the signal bandwidth B , i.e., $BT \ll 1$. Therefore, collect the received signal into a vector with N time slots, and we have

$$\begin{aligned} \mathbf{r}(t) & \triangleq [r_0(t), r_1(t), \dots, r_{N-1}(t)]^T \quad (6) \\ & = \mathbf{w}(t) + \sum_{k=0}^{K-1} \frac{\gamma \alpha_k}{d_{\text{AT},k} d_{\text{TR},k} d_{\text{RS}}} s(t - \tau_{\text{ATRS},k}) \\ & \quad \sum_{m=0}^{M-1} e^{j \frac{2\pi m d_{\text{E}}}{\lambda} \sin(\theta_{\text{RS}} + \sin \theta_{\text{TR},k})} \mathbf{g}_m \\ & \quad + \frac{\gamma \beta}{d_{\text{AR}} d_{\text{RS}}} s(t - \tau_{\text{ARS}}) \sum_{m=0}^{M-1} e^{j \frac{2\pi m d_{\text{E}}}{\lambda} \sin(\theta_{\text{RS}} + \theta_{\text{AR}})} \mathbf{g}_m \\ & = \sum_{k=0}^{K-1} \frac{\gamma \alpha_k}{d_{\text{AT},k} d_{\text{TR},k} d_{\text{RS}}} s(t - \tau_{\text{ATRS},k}) \mathbf{G} \mathbf{a}(\theta_{\text{TR},k}) \\ & \quad + \frac{\gamma \beta}{d_{\text{AR}} d_{\text{RS}}} s(t - \tau_{\text{ARS}}) \mathbf{G} \mathbf{a}(\theta_{\text{AR}}) + \mathbf{w}(t) \end{aligned}$$

where we define $\mathbf{w}(t) \triangleq [w_0(t), w_1(t), \dots, w_{N-1}(t)]^T$, $g_{m,n} \triangleq A_{m,n} e^{j \phi_{m,n}}$, $\mathbf{g}_m \triangleq [g_{m,0}, g_{m,1}, \dots, g_{m,N-1}]^T$, and the measurement matrix is defined as $\mathbf{G} \triangleq [\mathbf{g}_0, \mathbf{g}_1, \dots, \mathbf{g}_{M-1}] \in \mathbb{C}^{N \times M}$. We also define the steering vector as

$$\mathbf{a}(\theta) \triangleq \left[1, e^{j \frac{2\pi d_{\text{E}}}{\lambda} \sin(\theta_{\text{RS}} + \theta)}, \dots, e^{j \frac{2\pi (M-1) d_{\text{E}}}{\lambda} \sin(\theta_{\text{RS}} + \theta)} \right]^T. \quad (7)$$

By defining $z_k(t) \triangleq \frac{\gamma \alpha_k}{d_{\text{AT},k} d_{\text{TR},k} d_{\text{RS}}} s(t - \tau_{\text{ATRS},k})$, we have $\mathbf{z}(t) \triangleq [z_0(t), z_1(t), \dots, z_{K-1}(t)]^T$. Additionally, we also define $q(t) \triangleq \frac{\gamma \beta}{d_{\text{AR}} d_{\text{RS}}} s(t - \tau_{\text{ARS}})$. Finally, the received signal in the sensor can be simplified in a vector form

$$\mathbf{r}(t) = \mathbf{G} \mathbf{A}(\theta_{\text{TR}}) \mathbf{z}(t) + \mathbf{G} \mathbf{a}(\theta_{\text{AR}}) q(t) + \mathbf{w}(t), \quad (8)$$

where we define

$$\mathbf{A}(\theta_{\text{TR}}) \triangleq [\mathbf{a}(\theta_{\text{TR},0}), \mathbf{a}(\theta_{\text{TR},1}), \dots, \mathbf{a}(\theta_{\text{TR},K-1})] \in \mathbb{C}^{M \times K}. \quad (9)$$

In the system model (8), since the passive sensing method is considered, the measurement matrix \mathbf{G} in the RIS and the received signal $\mathbf{r}(t)$ are known. However, the signals $\mathbf{z}(t)$ and the interference $q(t)$ are unknown. We are trying to estimate the DOA vector θ_{TR} from the received signal $\mathbf{r}(t)$.

III. THE SPARSE-BASED DOA ESTIMATION METHOD

A. The Atomic Norm Minimization-Based Denoising Method

From the received signal (8), we can find that the target echoed signals are interfered by the direct signal from the AP to the RIS, and the direct signal is also unknown in the passive sensing system. Therefore, we propose a novel method based on the ANM with the interference cancellation. In the following contents, the parameter t has been ignored for simplification. The sensing problem can be formulated as

$$\min_{\xi, \eta} \|\mathbf{r} - \mathbf{G}\xi - \mathbf{G}\mathbf{a}(\theta_{\text{AR}})\eta\|_2^2 + \rho\|\xi\|_{\mathcal{A}}, \quad (10)$$

where $\eta \in \mathbb{C}$ and $\xi \in \mathbb{C}^{M \times 1}$. In practical, the value of ρ can be chosen as $\rho = \sigma_w \sqrt{M \log M}$ [30].

The optimization problem (10) can be rewritten as

$$\begin{aligned} & \min_{\xi, \eta} \|\xi\|_{\mathcal{A}} \\ & \text{s.t. } \|\mathbf{r} - \mathbf{G}\xi - \mathbf{G}\mathbf{a}(\theta_{\text{AR}})\eta\|_2^2 \leq \rho'. \end{aligned} \quad (11)$$

The corresponding Lagrangian function with dual variable $\bar{\rho}$ can be expressed as

$$\begin{aligned} \mathcal{L}(\xi, \eta, \bar{\rho}) &= \|\xi\|_{\mathcal{A}} + \bar{\rho}(\|\mathbf{r} - \mathbf{G}\xi - \mathbf{G}\mathbf{a}(\theta_{\text{AR}})\eta\|_2^2 - \rho') \\ &= \|\mathbf{r} - \mathbf{G}\xi - \mathbf{G}\mathbf{a}(\theta_{\text{AR}})\eta\|_2^2 + 1/\bar{\rho}(\|\xi\|_{\mathcal{A}} - \bar{\rho}\rho') \end{aligned} \quad (12)$$

To solve the optimization problem (10), the ANM-based method is proposed. The optimization problem can be rewritten as

$$\min_{\xi, \eta} \|\mathbf{r} - \mathbf{G}\xi - \mathbf{G}\mathbf{a}(\theta_{\text{AR}})\eta\|_2^2 + \rho\|\xi\|_{\mathcal{A}}, \quad (13)$$

where $\|\xi\|_{\mathcal{A}}$ is the atomic norm of ξ , and is defined as

$$\|\xi\|_{\mathcal{A}} \triangleq \inf \{c \geq 0 : \xi \in c \cdot \text{conv}\{\mathbb{A}\}\}. \quad (14)$$

\mathbb{A} is an atomic set for the DOA estimation, and is defined as

$$\mathbb{A} = \{e^{j\phi_{\mathbb{A}}} \mathbf{a}(\theta) : \theta \in [-\pi/2, \pi/2], \phi_{\mathbb{A}} \in [0, 2\pi]\}. \quad (15)$$

The optimization problem (13) cannot be solved directly, we first obtain the following atomic norm expression

$$\|\xi\|_{\mathcal{A}} = \inf \left\{ \sum_p c_p : \xi = \sum_p c_p \mathbf{a}_p, c_p \geq 0, \mathbf{a}_p \in \mathbb{A} \right\}. \quad (16)$$

According to [31]–[33], the atomic norm can be also obtained by an equivalent semidefinite program (SDP) problem

$$\begin{aligned} \|\xi\|_{\mathcal{A}} &= \inf_{\mathbf{u}, \nu} \left\{ \frac{1}{2N} \text{Tr}\{\text{Toep}(\mathbf{u})\} + \frac{1}{2}\nu : \right. \\ &\quad \left. \begin{bmatrix} \text{Toep}(\mathbf{u}), & \xi \\ \xi^H, & \nu \end{bmatrix} \succeq 0 \right\}, \end{aligned} \quad (17)$$

where $\mathbf{u} \in \mathbb{C}^{M \times 1}$ and $\text{Toep}(\mathbf{u})$ denotes a Toeplitz matrix with the first column being \mathbf{u} and can be expressed as

$$\text{Toep}(\mathbf{u}) \triangleq \begin{bmatrix} u_0 & u_{-1} & \dots & u_{-(M-1)} \\ u_1 & u_0 & \dots & u_{-(M-2)} \\ \vdots & \vdots & \ddots & \vdots \\ u_{M-1} & u_{M-2} & \dots & u_0 \end{bmatrix}. \quad (18)$$

Hence, by defining $\mathbf{b} \triangleq \mathbf{G}\mathbf{a}(\theta_{\text{AR}}) \in \mathbb{C}^{N \times 1}$, the optimization problem in (10) can be rewritten as

$$\begin{aligned} & \min_{\xi, \mathbf{u}, \nu, \eta} \|\mathbf{r} - \mathbf{G}\xi - \eta\mathbf{b}\|_2^2 + \frac{\rho}{2} \left[\frac{1}{M} \text{Tr}\{\text{Toep}(\mathbf{u})\} + \nu \right] \\ & \text{s.t. } \begin{bmatrix} \text{Toep}(\mathbf{u}), & \xi \\ \xi^H, & \nu \end{bmatrix} \succeq 0. \end{aligned} \quad (19)$$

By solving the SDP problem, the denoising vector ξ can be obtained.

B. The Hankel-Based MUSIC Method for the Spatial Spectrum Estimation

With the SDP problem (19), we can reconstruct the signal ξ with the sparsity priority. However, the signal ξ is sparse in the frequency domain, and the DOA vector θ_{TR} is still unknown. We will use a MUSIC-based method to estimate the DOA without discretizing the spatial domain into grids. Since the reconstruction signal $\xi \in \mathbb{C}^{M \times 1}$ is a vector, the covariance matrix cannot be obtained with only one snapshot. The traditional MUSIC cannot be used directly, so a Hankel matrix-based method is proposed to realize a MUSIC-based method [34]. First, a Hankel matrix is obtained as

$$\text{Hankel}(\xi) = \begin{bmatrix} \xi_{0:M-L}^T \\ \xi_{1:1+M-L}^T \\ \vdots \\ \xi_{L-1:M-1}^T \end{bmatrix}, \quad (20)$$

where $\xi_{m':n'}$ denotes a sub-vector of ξ using the m' -th to the n' -th entries. We reshape a vector ξ using M elements to a matrix using L elements.

Then, a singular value decomposition (SVD) is adopted to obtain the noise subspace, and we have

$$\text{Hankel}(\xi) = \mathbf{U}_1 \mathbf{D} \mathbf{U}_2, \quad (21)$$

where \mathbf{D} is a matrix with the diagonal entries being the singular values. \mathbf{U}_1 and \mathbf{U}_2 are the complex unitary matrices. The columns of \mathbf{U}_1 and \mathbf{U}_2 are the left-singular and right-singular vectors, respectively.

The noise subspace can be obtained as $\tilde{\mathbf{U}}$ from the columns of \mathbf{U}_1 corresponding to the small singular values. Finally, the spatial spectrum with only one snapshot can be obtained as

$$g_{\text{sp}}(\theta) = \frac{\|\tilde{\mathbf{a}}(\theta)\|_2^2}{\|\tilde{\mathbf{a}}^H(\theta)\tilde{\mathbf{U}}\|_2^2}, \quad (22)$$

where we define a steering vector for sub-array as

$$\tilde{\mathbf{a}}(\theta) \triangleq \left[1, e^{j\frac{2\pi d_E}{\lambda} \sin(\theta_{\text{RS}} + \theta)}, \dots, e^{j\frac{2\pi(L-1)d_E}{\lambda} \sin(\theta_{\text{RS}} + \theta)} \right]^T. \quad (23)$$

The DOA θ_{TR} can be estimated by finding the peak values of $g_{\text{sp}}(\theta)$. The details of the proposed method is summarized in Algorithm 1. The computational complexity of the proposed method is determined by the SDP and SVD steps. The computational complexity of SDP step is about $\mathcal{O}((M+1)^4)$, and that of SVD is about $\mathcal{O}(L^2(M-L+1) + M(M-L+1)^2 + (M-L+1)^3)$. Since $M > L$, the computational complexity of Algorithm 1 is about $\mathcal{O}((M+1)^4)$.

Algorithm 1 ANM-PDOA: Atomic norm-based passive DOA estimation method for the RIS-based sensing system

1: *Input*: The received signal r , the measurement matrix G , the direction θ_{RS} between the RIS and the sensor, the direction θ_{AR} between the AP and the RIS, the number of RIS elements M , the wavelength λ , the distance between the adjacent RIS elements d_{E} , and the size L of sub-array.

2: Define the steering vector as

$$\mathbf{a}(\theta) \triangleq \left[1, \dots, e^{j \frac{2\pi(M-1)d_{\text{E}}}{\lambda} \sin(\theta_{\text{RS}} + \theta)} \right]^T. \quad (24)$$

3: Obtain \mathbf{b} from $\mathbf{b} = G\mathbf{a}(\theta_{\text{AR}})$.

4: Obtain ξ from

$$\begin{aligned} \min_{\xi, u, \nu, \eta} & \|r - G\xi - \eta\mathbf{b}\|_2^2 + \frac{\rho}{2} \left[\frac{1}{M} \text{Tr}\{\text{Toep}(\mathbf{u})\} + \nu \right] \\ \text{s.t.} & \begin{bmatrix} \text{Toep}(\mathbf{u}), & \xi \\ \xi^H, & \nu \end{bmatrix} \succeq 0. \end{aligned} \quad (25)$$

5: Obtain a Hankel matrix from

$$\text{Hankel}(\xi) = [\xi_{0:M-L}, \dots, \xi_{L-1:M-1}]^T. \quad (26)$$

6: The SVD is used as $\text{Hankel}(\xi) = \mathbf{U}_1 \mathbf{D} \mathbf{U}_2$.

7: Obtain the noise subspace can be obtained as $\tilde{\mathbf{U}}$ from the columns of \mathbf{U}_1 corresponding to the small singular values.

8: Define the steering vector of a sub-array as

$$\tilde{\mathbf{a}}(\theta) \triangleq \left[1, \dots, e^{j \frac{2\pi(L-1)d_{\text{E}}}{\lambda} \sin(\theta_{\text{RS}} + \theta)} \right]^T. \quad (27)$$

9: The spatial spectrum is obtained as

$$g_{\text{sp}}(\theta) = \frac{\|\tilde{\mathbf{a}}(\theta)\|_2^2}{\|\tilde{\mathbf{a}}^H(\theta)\tilde{\mathbf{U}}\|_2^2}, \quad (28)$$

10: The DOA $\hat{\theta}_{\text{TR}}$ can be estimated from the peak values of $g_{\text{sp}}(\theta)$.

11: *Output*: The estimated DOA $\hat{\theta}_{\text{TR}}$.

IV. OPTIMIZING THE MEASUREMENT MATRIX

From the system model (8), we can find that the SINR of the received signal can be expressed as

$$g_{\text{SINR}}(\mathbf{G}) = \frac{\mathcal{E} \{ \|G\mathbf{A}(\theta_{\text{TR}})\mathbf{z}(t)\|_2^2 \}}{\mathcal{E} \{ \|G\mathbf{a}(\theta_{\text{AR}})q(t)\|_2^2 \} + \mathcal{E} \{ \|\mathbf{w}(t)\|_2^2 \}}, \quad (29)$$

which can be simplified as

$$g_{\text{SINR}}(\mathbf{G}) = \frac{\text{Tr} \{ G\mathbf{A}(\theta_{\text{TR}})\Lambda\mathbf{A}^H(\theta_{\text{TR}})G^H \}}{\|\mathbf{G}\mathbf{a}(\theta_{\text{AR}})\|_2^2 \left| \frac{\gamma\beta}{d_{\text{AR}}d_{\text{RS}}} \right|^2 P_s + N\sigma_w^2}, \quad (30)$$

and $\Lambda \triangleq \gamma^2 P_s \text{diag} \left\{ \left| \frac{\alpha_0}{d_{\text{AT},0}d_{\text{TR},0}d_{\text{RS}}} \right|^2, \dots, \left| \frac{\alpha_{K-1}}{d_{\text{AT},K-1}d_{\text{TR},K-1}d_{\text{RS}}} \right|^2 \right\}$

Hence, we can optimize the measurement matrix \mathbf{G} to improve the SINR of the received signal. In the practical

sensing system, the targets can be at any directions, so the DOA vector θ_{TR} is unknown. To improve the SINR of the received signal, we can just decrease the power from the AP, so the following optimization problem can be formulated

$$\begin{aligned} \min_{\mathbf{G}} & \|\mathbf{G}\mathbf{a}(\theta_{\text{AR}})\|_2^2 \left| \frac{\gamma\beta}{d_{\text{AR}}d_{\text{RS}}} \right|^2 P_s + N\sigma_w^2 \\ \text{s.t.} & |g_{m,n}| \leq 1. \end{aligned} \quad (31)$$

To solve the optimization problem (31), we rewrite the measurement matrix as $\mathbf{G} = [\mathbf{g}_0', \mathbf{g}_1', \dots, \mathbf{g}_{N-1}']^H$, so we can optimize the row of \mathbf{G} iterative. For the n -th row, we can formulate the following problem

$$\begin{aligned} \min_{\mathbf{g}'_n} & \|\mathbf{g}'_n \mathbf{a}(\theta_{\text{AR}})\|_2^2 \\ \text{s.t.} & |g'_{m,n}| \leq 1. \end{aligned} \quad (32)$$

Since we have

$$\|\mathbf{g}'_n \mathbf{a}(\theta_{\text{AR}})\|_2^2 = \text{Tr}\{\mathbf{a}(\theta_{\text{AR}})\mathbf{a}^H(\theta_{\text{AR}})\mathbf{g}'_n \mathbf{g}'_n^H\}, \quad (33)$$

the optimization problem (32) can be approximated by the following SDP problem

$$\begin{aligned} \min_{\tilde{\mathbf{G}}} & \text{Tr}\{\mathbf{a}(\theta_{\text{AR}})\mathbf{a}^H(\theta_{\text{AR}})\tilde{\mathbf{G}}\} \\ \text{s.t.} & \tilde{G}_{m,m} = 1 \ (m = 0, 1, \dots, M-1) \\ & \tilde{\mathbf{G}} \succeq 0 \\ & \tilde{\mathbf{G}} \text{ is a Hermitian matrix,} \end{aligned} \quad (34)$$

where $\tilde{G}_{m,m}$ denotes the m -th diagonal entry of $\tilde{\mathbf{G}}$, and we force on optimizing the phases of the RIS elements.

The problem (34) is convex and can be solved efficiently, and we can obtain a matrix $\tilde{\mathbf{G}}$. Since the measurement matrix \mathbf{G} must have the random characteristic to guarantee the sparse reconstruction performance. With eigenvalue decomposition [35], we have

$$\tilde{\mathbf{G}} = \tilde{\mathbf{U}} \tilde{\Lambda} \tilde{\mathbf{U}}^H, \quad (35)$$

and the n -th row can be chosen as

$$\mathbf{g}'_n = e^{j \text{ang}\{\tilde{\mathbf{U}} \tilde{\Lambda}^{\frac{1}{2}} \tilde{\mathbf{g}}\}}, \quad (36)$$

where $\text{ang}(\cdot)$ obtains the angle of a variable, and $\tilde{\mathbf{g}}$ is a random vector with the entries following the complex Gaussian distribution. The details to optimize the measurement matrix are given in Algorithm 2.

From the details of Algorithm 2, we can find that the computational complexity is determined by solving the SDP problem. Hence, the computational complexity of the proposed method is about $\mathcal{O}(M^4)$, where M is the number of the RIS elements.

V. THE CRLB FOR THE PASSIVE DOA ESTIMATION WITH RIS

The sensing performance using RIS can be measured by CRLB [36]–[38]. Collect all the unknown parameters into a vector

$$\zeta \triangleq [\theta_{\text{TR}}^T, \mathbf{z}^T(t), q(t)]^T, \quad (41)$$

Algorithm 2 The optimization method for the measurement matrix

- 1: *Input*: The direction θ_{RS} between the RIS and the sensor, the direction θ_{AR} between the AP and the RIS, and the number of RIS elements M .
- 2: Obtain the steering vector $\mathbf{a}(\theta_{\text{AR}})$ as

$$\mathbf{a}(\theta_{\text{AR}}) \triangleq \left[1, \dots, e^{j \frac{2\pi(M-1)d_{\text{E}}}{\lambda} \sin(\theta_{\text{RS}} + \theta_{\text{AR}})} \right]^T. \quad (37)$$

- 3: Obtain a Hermitian matrix $\tilde{\mathbf{G}}$ from

$$\min_{\tilde{\mathbf{G}}} \text{Tr}\{\mathbf{a}(\theta_{\text{AR}})\mathbf{a}^H(\theta_{\text{AR}})\tilde{\mathbf{G}}\} \quad (38)$$

$$\text{s.t. } \tilde{\mathbf{G}}_{m,m} = 1 \ (m = 0, 1, \dots, M-1)$$

$$\tilde{\mathbf{G}} \succeq 0$$

$\tilde{\mathbf{G}}$ is a Hermitian matrix.

- 4: Use the eigenvalue decomposition $\tilde{\mathbf{G}} = \tilde{\mathbf{U}}\tilde{\Lambda}\tilde{\mathbf{U}}^H$.

- 5: Generate a random vector $\tilde{\mathbf{g}}$ following the complex Gaussian distribution.

- 6: Obtain a vector \mathbf{g}'_n ($n = 0, 1, \dots, N-1$) as

$$\mathbf{g}'_n = e^{j \text{ang}\{\tilde{\mathbf{U}}\tilde{\Lambda}^{\frac{1}{2}}\tilde{\mathbf{g}}\}}. \quad (39)$$

- 7: Generate the measurement matrix as

$$\mathbf{G} = [\mathbf{g}'_0, \mathbf{g}'_1, \dots, \mathbf{g}'_{N-1}]^H. \quad (40)$$

- 8: *Output*: The measurement matrix \mathbf{G} .

and the probability density function of the received signal can be expressed as

$$f(\mathbf{r}(t); \zeta) = \frac{1}{\pi^N \det(\Sigma)} e^{-[\mathbf{r}(t) - \mu(t)]^H \Sigma^{-1} [\mathbf{r}(t) - \mu(t)]}, \quad (42)$$

where the mean μ and covariance matrix Σ are respectively

$$\mu = \mathbf{G}\mathbf{A}(\theta_{\text{TR}})\mathbf{z}(t) + \mathbf{G}\mathbf{a}(\theta_{\text{AR}})q(t), \quad (43)$$

$$\Sigma = \sigma_w^2 \mathbf{I}_N. \quad (44)$$

We denote the variance of noise as σ_w^2 .

To obtain the CRLB, the Fisher information matrix (FIM) can be calculated firstly, and is defined as \mathbf{F} . With the likelihood function $\ln f(\mathbf{r}(t); \zeta)$, we have

$$\begin{aligned} \frac{\partial \ln f(\mathbf{r}(t); \zeta)}{\partial \theta_{\text{TR}}} &= \frac{\partial \ln \frac{1}{\pi^N \det(\Sigma)} e^{-[\mathbf{r}(t) - \mu(t)]^H \Sigma^{-1} [\mathbf{r}(t) - \mu(t)]}}{\partial \theta_{\text{TR}}} \\ &= -\frac{\partial [\mathbf{r}(t) - \mu(t)]^H \Sigma^{-1} [\mathbf{r}(t) - \mu(t)]}{\partial \theta_{\text{TR}}} \\ &= 2\mathcal{R} \left\{ [\mathbf{r}(t) - \mu(t)]^H \Sigma^{-1} \mathbf{G} \frac{\partial \mathbf{A}(\theta_{\text{TR}})\mathbf{z}(t)}{\partial \theta_{\text{TR}}} \right\} \\ &= 2\mathcal{R} \left\{ [\mathbf{r}(t) - \mu(t)]^H \Sigma^{-1} \mathbf{G}\mathbf{B} \right\}, \end{aligned} \quad (45)$$

where the k -th ($k = 0, 1, \dots, K-1$) column of \mathbf{B} is

$$\begin{aligned} \mathbf{b}(\theta_{\text{TR},k}) &= z_k(t) \frac{\partial \mathbf{a}(\theta_{\text{TR},k})}{\partial \theta_{\text{TR},k}} \\ &= j \frac{2\pi d_{\text{E}} z_k(t)}{\lambda} \cos(\theta_{\text{RS}} + \theta_{\text{TR},k}) [\mathbf{a}(\theta_{\text{TR},k}) \odot \mathbf{l}_M], \end{aligned} \quad (46)$$

and we define

$$\mathbf{l}_M = [0, 1, \dots, M-1]^T. \quad (47)$$

Additionally, we also have

$$\begin{aligned} \frac{\partial \ln f(\mathbf{r}(t); \zeta)}{\partial \mathbf{z}(t)} &= \frac{\partial \ln \frac{1}{\pi^N \det(\Sigma)} e^{-[\mathbf{r}(t) - \mu(t)]^H \Sigma^{-1} [\mathbf{r}(t) - \mu(t)]}}{\partial \mathbf{z}(t)} \\ &= -\frac{\partial [\mathbf{r}(t) - \mu(t)]^H \Sigma^{-1} [\mathbf{r}(t) - \mu(t)]}{\partial \mathbf{z}(t)} \\ &= [\mathbf{r}(t) - \mu(t)]^H \Sigma^{-1} \frac{\partial \mathbf{G}\mathbf{A}(\theta_{\text{TR}})\mathbf{z}(t)}{\partial \mathbf{z}(t)} \\ &\quad + \{\Sigma^{-1}[\mathbf{r}(t) - \mu(t)]\}^T \frac{\partial [\mathbf{G}\mathbf{A}(\theta_{\text{TR}})\mathbf{z}(t)]^*}{\partial \mathbf{z}(t)} \\ &= [\mathbf{r}(t) - \mu(t)]^H \Sigma^{-1} \mathbf{G}\mathbf{A}(\theta_{\text{TR}}). \end{aligned} \quad (48)$$

For the unknown signal $q(t)$, we have

$$\begin{aligned} \frac{\partial \ln f(\mathbf{r}(t); \zeta)}{\partial q(t)} &= \frac{\partial \ln \frac{1}{\pi^N \det(\Sigma)} e^{-[\mathbf{r}(t) - \mu(t)]^H \Sigma^{-1} [\mathbf{r}(t) - \mu(t)]}}{\partial q(t)} \\ &= -\frac{\partial [\mathbf{r}(t) - \mu(t)]^H \Sigma^{-1} [\mathbf{r}(t) - \mu(t)]}{\partial q(t)} \\ &= [\mathbf{r}(t) - \mu(t)]^H \Sigma^{-1} \frac{\partial \mu(t)}{\partial q(t)} \\ &\quad + \{\Sigma^{-1}[\mathbf{r}(t) - \mu(t)]\}^T \frac{\partial \mu^*(t)}{\partial q(t)} \\ &= [\mathbf{r}(t) - \mu(t)]^H \Sigma^{-1} \mathbf{G}\mathbf{a}(\theta_{\text{AR}}). \end{aligned} \quad (49)$$

Therefore, the FIM can be obtained as

$$\mathbf{F} = \begin{bmatrix} \Omega_{1,1} & \Omega_{1,2} & \Omega_{1,3} \\ \Omega_{2,1} & \Omega_{2,2} & \Omega_{2,3} \\ \Omega_{3,1} & \Omega_{3,2} & \Omega_{3,3} \end{bmatrix}. \quad (50)$$

The expressions are given in Appendix A. Finally, the expression for FIM can be expressed as (51).

The CRLB for the DOA estimation of the k -th target can be expressed as

$$f_{\text{CRLB}}(\theta_{\text{TR},k}) \geq [\mathbf{F}^{-1}]_{k,k}. \quad (52)$$

where $[A]_{m,n}$ denotes an entry of \mathbf{A} at the m -th row and n -th column.

We give a simple example of CRLB for only one target with the DOA being ψ , and the CRLB can be expressed as

$$\begin{aligned} f_{\text{CRLB}}(\psi) &\geq [\mathbf{F}^{-1}]_{0,0} \geq \frac{\sigma_w^2}{2\mathcal{R}\{\mathbf{B}^H \mathbf{G}^H \mathbf{G}\mathbf{B}\}} \\ &= \frac{\sigma_w^2}{2\mathbf{b}^H(\psi) \mathbf{G}^H \mathbf{G}\mathbf{b}(\psi)} \\ &= \frac{\sigma_w^2}{2|z(t)|^2 \nabla_{\psi} \mathbf{a}^H(\psi) \mathbf{G}^H \mathbf{G} \nabla_{\psi} \mathbf{a}(\psi)} \\ &= \frac{\sigma_w^2 d_{\text{AT}}^2 d_{\text{TR}}^2 d_{\text{RS}}^2}{2|\gamma\alpha|^2 P_s} \|\mathbf{G} \nabla_{\psi} \mathbf{a}(\psi)\|_2^{-2} \end{aligned} \quad (53)$$

$$\mathbf{F} = \sigma_w^{-2} \begin{bmatrix} 2\mathcal{R}\{\mathbf{B}^H \mathbf{G}^H \mathbf{G} \mathbf{B}\} & \mathbf{B}^H \mathbf{G}^H \mathbf{G} \mathbf{A}(\theta_{\text{TR}}) & \mathbf{B}^H \mathbf{G}^H \mathbf{G} \mathbf{a}(\theta_{\text{AR}}) \\ \mathbf{A}^H(\theta_{\text{TR}}) \mathbf{G}^H \mathbf{G} \mathbf{B} & \mathbf{A}^H(\theta_{\text{TR}}) \mathbf{G}^H \mathbf{G} \mathbf{A}(\theta_{\text{TR}}) & \mathbf{A}^H(\theta_{\text{TR}}) \mathbf{G}^H \mathbf{G} \mathbf{a}(\theta_{\text{AR}}) \\ \mathbf{a}^H(\theta_{\text{AR}}) \mathbf{G}^H \mathbf{G} \mathbf{B} & \mathbf{a}^H(\theta_{\text{AR}}) \mathbf{G}^H \mathbf{G} \mathbf{A}(\theta_{\text{TR}}) & \mathbf{a}^H(\theta_{\text{AR}}) \mathbf{G}^H \mathbf{G} \mathbf{a}(\theta_{\text{AR}}) \end{bmatrix}. \quad (51)$$

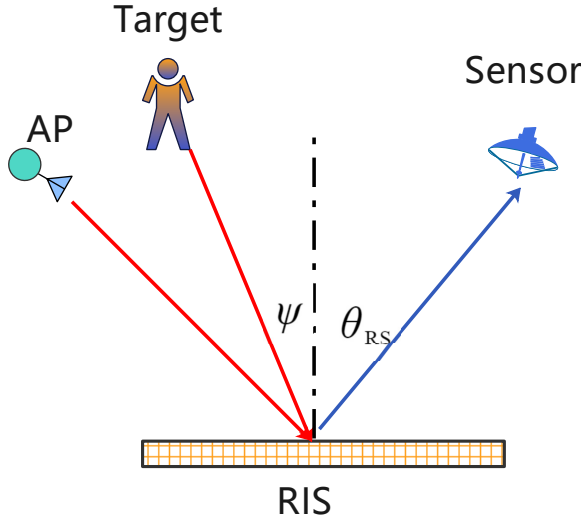


Fig. 2. The diagram to optimize the measurement matrix

where P_s is the power of the transmitted signal, α is determined by the target scattering coefficient, and γ is determined by the antenna gains of RIS and sensor. d_{AT} , d_{TR} and d_{RS} are the distance between the AP and the target, the distance between target and the RIS, and the distance between the RIS and the sensor, respectively.

Therefore, we can decrease the CRLB to improve the DOA estimation performance. The following methods can be done to improve the performance:

- 1) Decreasing the distance d_{AT} between the AP and target, the distance d_{TR} between the target and the RIS, and the distance d_{RS} between the RIS and the sensor;
- 2) Increasing the antenna gains of RIS and sensor;
- 3) Increasing ratio P_s/σ_w^2 between the transmitting power and noise;
- 4) Optimizing the measurement matrix \mathbf{G} to improve $\|\mathbf{G} \nabla_\psi \mathbf{a}(\psi)\|_2^2$.

For the practical consideration, we can design the system by putting the sensor closed to the RIS to decreasing d_{RS} , and optimize the measurement matrix \mathbf{G} . As shown in Fig. 2, we can optimize the measurement matrix \mathbf{G} correspond to the steering vector of the angle $\psi + \theta_{\text{RS}}$. For convenience, we can set $\theta_{\text{RS}} = 0$ to simplify the optimization of \mathbf{G} .

VI. SIMULATION RESULTS

In this section, simulation results for the proposed passive sensing in the system using the RIS are carried out in a personal computer with MATLAB R2020b, Intel Core i5 @ 2.9 GHz processor, and 8 GB LPDDR3 @ 2133 MHz. Additionally, the code about the proposed method is available online <https://github.com/chenpengseu/>

TABLE I
SIMULATION PARAMETERS

| Parameter | Value |
|--|--|
| The direction between the RIS and sensor | $\theta_{\text{RS}} = 0$ |
| The distance between adjacent elements | $d_E = 0.5\lambda$ |
| The number of RIS elements | $M = 64$ |
| The direction between the AP and RIS | $\theta_{\text{AR}} = -9.3878^\circ$ |
| The number of targets | $K = 3$ |
| The distance between the AP and targets | $d_{\text{AT}} = 20 \text{ m}$ |
| The distance between the RIS and targets | $d_{\text{TR}} = 30 \text{ m}$ |
| The distance between the RIS and sensor | $d_{\text{RS}} = 3 \text{ m}$ |
| The distance between the AP and RIS | $d_{\text{AR}} = 5 \text{ m}$ |
| The number of measurements | $N = 16$ |
| The spatial range | $[-45^\circ, 45^\circ]$ |
| The mean value of DOA | $\mathbb{E}\{\theta_{\text{TR}}\} = [-25^\circ, 15^\circ, 30^\circ]$ |

PassiveDOA-ISAC-RIS.git. The simulation parameters are given in Table I. Moreover, we also show the performance with methods with and without the grids. In the methods with grids, the spatial domain is discretized into grids with the grid size being 1° , and the methods without grids have a grid size being 0.01° .

First, we show the root mean squared error (RMSE, the root of CRLB root) of the DOA estimation performance in the scenarios with different positions of the AP and the sensor, where the noise variance is $\sigma_w^2 = 0.01$. In Fig. 3(a), the AP is at $(0 \text{ m}, 0 \text{ m})$, the RIS is at $(20 \text{ m}, 20 \text{ m})$, and the sensor is at $(20 \text{ m}, 0 \text{ m})$. The different colors show the low bound of the DOA estimation in RMSE, and we can find that the area closed to the AP and the RIS has better performance than other areas. The worse RMSE is about 25° in the interesting area. Additionally, we also show the estimation low bound in the scenario with the sensor at $(20 \text{ m}, 17 \text{ m})$ in Fig. 3(b), and we can find that the overall RMSE is less than 4° . Hence, better performance can be achieved by Fig. 3(b) than that by Fig. 3(a). Moreover, we move the AP to the position $(20 \text{ m}, 0 \text{ m})$ in Fig. 3(c), and move the AP to the position $(20 \text{ m}, -20 \text{ m})$ in Fig. 3(d). The area with better estimation performance is also moving with the AP. Fig. 3(d) achieves the best performance than other 3 scenarios. From the results in Fig. 3, we can find that a better estimation performance can be achieved by putting the sensor close to the RIS.

Second, for the DOA estimation, we show the estimated spatial spectrum in Fig. 4, and we also compare it with the following methods:

- FFT method: The traditional fast Fourier transformation (FFT) method estimates the spatial spectrum without discretizing the spatial domain, and the Rayleigh criterion limits the resolution.
- FFT (interference removal) method: In this paper, the

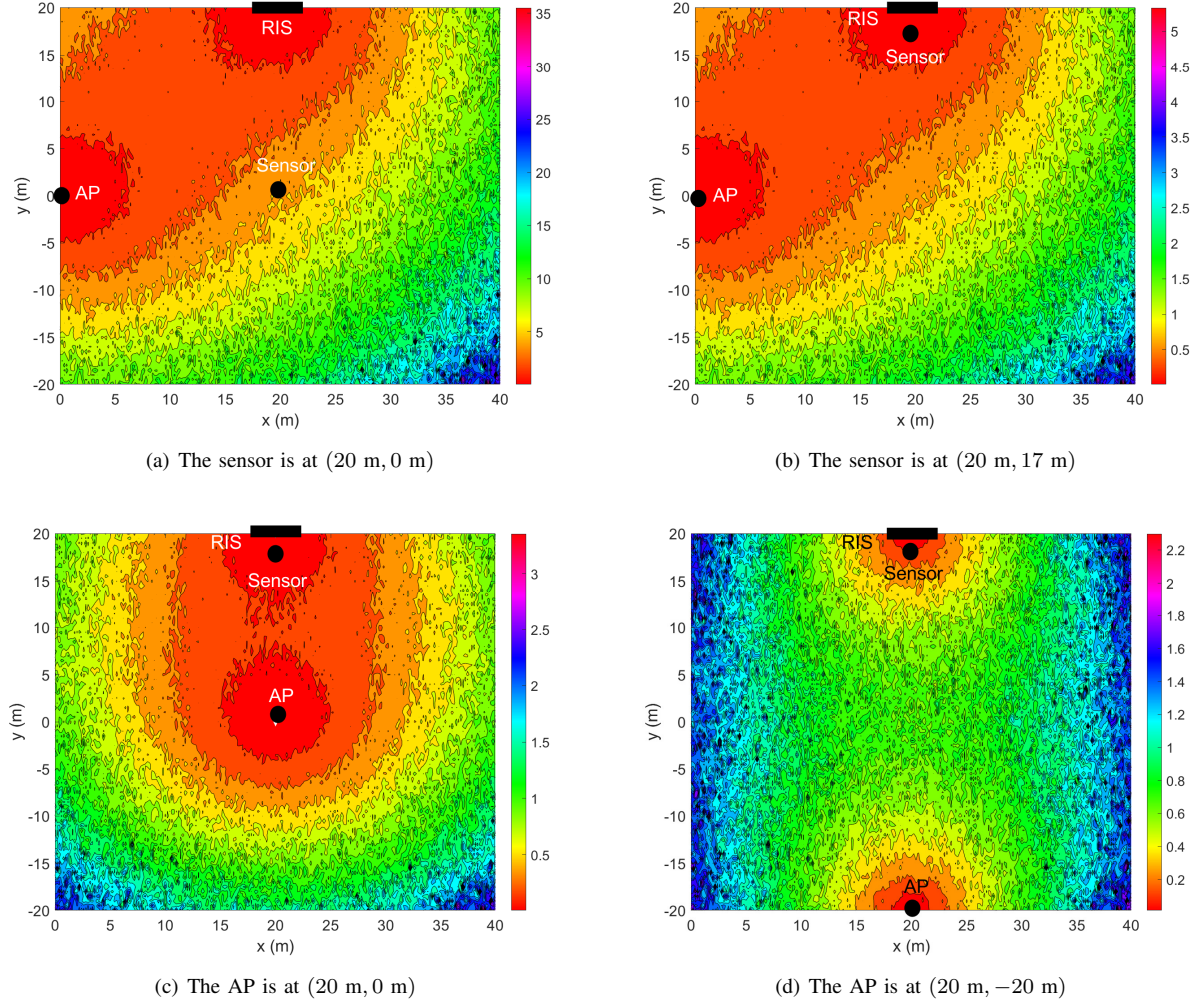


Fig. 3. The RMSE (root of CRLB) with different positions of the AP and the sensor.

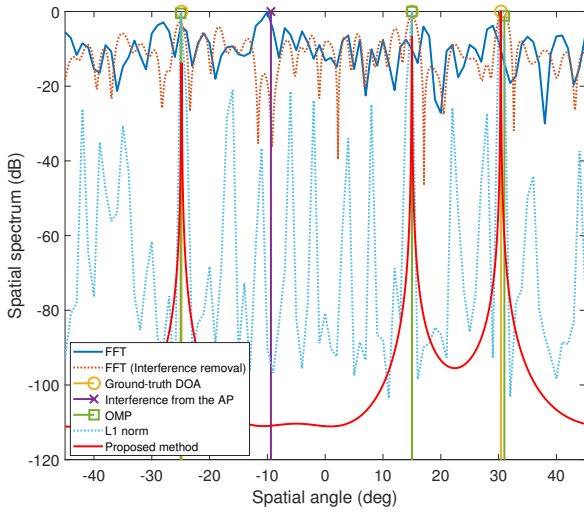


Fig. 4. The estimated spatial spectrum with SNR being 20 dB.

interference from the AP is estimated and removed first. Then, the FFT method is used to estimate the DOA of targets.

- OMP method [39]–[41]: OMP method is a grid-based method for sparse reconstruction, where the interference from the AP is removed first. The OMP method has lower computational complexity in the scenario with fewer grids but higher with more grids, where a matrix inverse determines the complexity at the iterative step.
- ℓ_1 norm method [42,43]: The ℓ_1 norm minimization method is a convex optimization method for the sparse reconstruction, and we formulate the ℓ_1 norm method as follows:

$$\min_{\tilde{\mathbf{x}}, \tilde{q}} \left\| \mathbf{r} - \mathbf{G} \tilde{\mathbf{D}} \tilde{\mathbf{x}} - \mathbf{G} \mathbf{a}(\theta_{\text{AR}}) \tilde{q} \right\|_2^2 + \tilde{\rho} \|\tilde{\mathbf{x}}\|_1, \quad (54)$$

where $\tilde{\rho}$ is a parameter to control the balance between the sparsity and the reconstruction error, $\tilde{\mathbf{x}}$ is the sparse spectrum, \tilde{q} is the interference from the AP, and $\tilde{\mathbf{D}}$ denotes the Fourier dictionary matrix for the ℓ_1 reconstruction.

As shown in Fig. 4, with the SNR being 20 dB, the FFT and the FFT (interference removal) methods cannot estimate

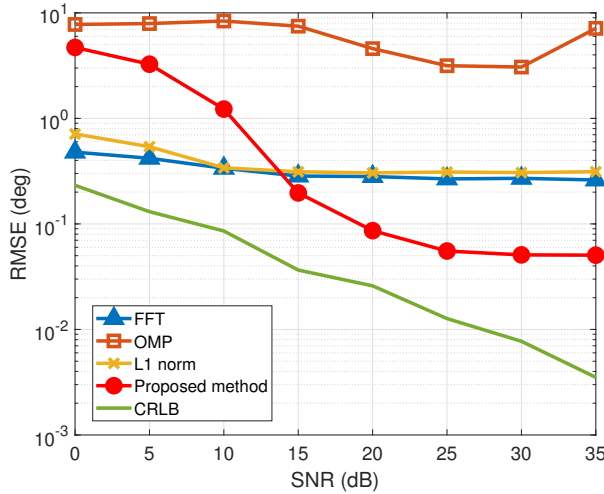


Fig. 5. The estimated performance with different SNRs (without measurement matrix optimization).

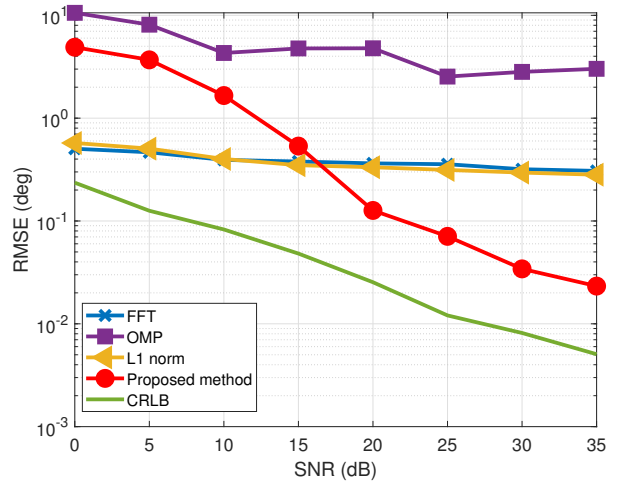


Fig. 7. The estimated performance with different SNRs (with measurement matrix optimization).

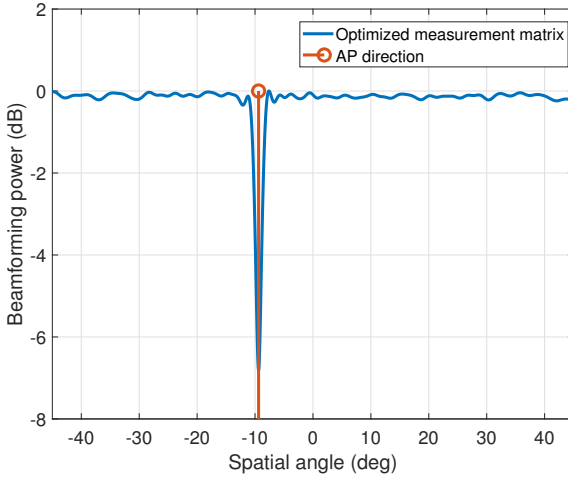


Fig. 6. The beamforming results using the optimized measurement matrix.

the spatial spectrum well, since the number of measurements N is much less than the number of RIS elements M . The proposed method, the ℓ_1 norm method and the OMP method can estimate the DOA well. Additionally, the proposed method can achieve better estimation performance than other methods.

Then, we show the DOA estimation performance in the scenario with different SNRs in Fig. 5, where the measurement matrix is chosen randomly and not optimized. We can find that the proposed method can outperform the existing methods when the SNR is greater than 15 dB, where the RMSE is less than 0.2° . However, with the improvement of SNR, the estimation performance cannot be improved when the SNR is greater than 25 dB, where the RMSE is about 0.05° . The RMSE platform is caused by interference from the AP.

Moreover, we use the proposed method to optimize the measurement matrix. With the optimized matrix \mathbf{G} , the beamforming results are shown in Fig. 6. We can find that the

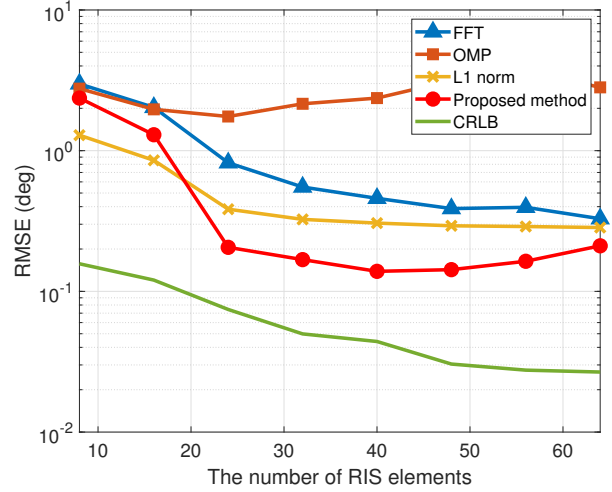


Fig. 8. The estimation performance with different numbers of RIS elements (the SNR is 20 dB).

beam power from the direction of the AP is much less than in other directions, so that the interference can be removed significantly. Then, we use the optimized matrix \mathbf{G} to perform the DOA estimation, and the estimation performance is shown in Fig. 7. The better estimation performance is achieved in the scenario with $\text{SNR} \geq 20$ dB. Furthermore, the RMSE platform is also broken, and the performance can achieve the CRLB with the increasing SNR.

The DOA estimation performance with different numbers of RIS elements is shown in Fig. 8, and we can find that the better estimation performance is achieved by the proposed method in the scenario with $M \geq 24$. However, the estimation performance cannot be further improved with more elements. Hence, in the proposed passive sensing system, we can choose a suitable number of elements, and the performance improvement with more elements is limited.

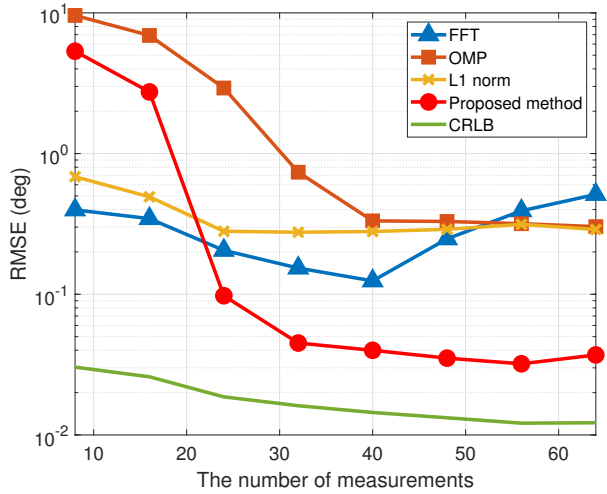


Fig. 9. The estimation performance with different numbers of measurements (the SNR is 20 dB).

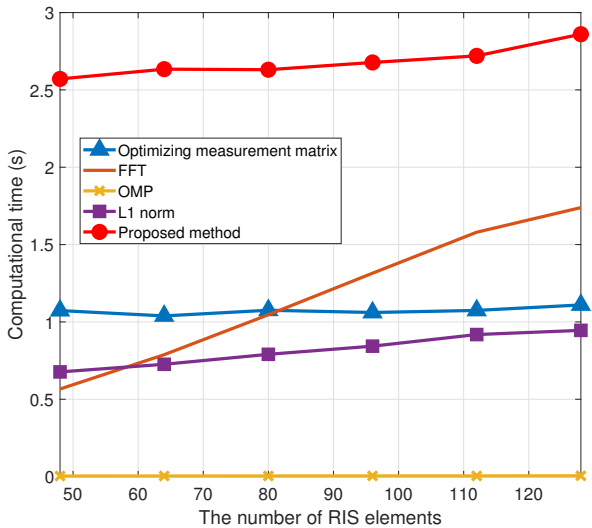


Fig. 10. The computational time with different numbers of RIS elements.

For the different numbers N of measurements, the estimation performance is shown in Fig. 9. More measurements can improve the estimation performance. For the proposed method, the performance cannot be further improved when $N \geq 32$, where the RMSE is about 0.04° . For the OMP method, the RMSE platform is about 0.3° . Hence, the proposed method is much better than the existing methods. Finally, the computational time of the proposed method is shown in Fig. 10. The computational time increases with more RIS elements when the proposed method and the FFT method are adopted. The computational time of the proposed method is about 2.6 s, and is acceptable in most applications.

VII. CONCLUSIONS

The passive DOA estimation problem has been addressed in the proposed ISAC system with the RIS. The system model with the interference of wireless communication has been formulated. The atomic norm-based method has also been proposed for the DOA estimation with the interference removal, and the spatial spectrum has been estimated by the Hankel-based MUSIC method. Additionally, the optimization problem has been solved for the measurement matrix to remove the interference. The estimation performance has been measured by the CRLB, which can be used to optimize the distribution of the sensing node. The simulation results have shown the advantage of the proposed method in the DOA estimation. Future work will focus on sensing methods with lower computational complexity.

REFERENCES

- [1] X. Wang, Z. Fei, J. Huang, and H. Yu, "Joint waveform and discrete phase shift design for RIS-assisted integrated sensing and communication system under Cramer-Rao bound constraint," *IEEE Trans. Veh. Technol.*, vol. 71, no. 1, pp. 1004–1009, 2022.
- [2] J. A. Zhang, F. Liu, C. Masouros, R. W. Heath, Z. Feng, L. Zheng, and A. Petropulu, "An overview of signal processing techniques for joint communication and radar sensing," *IEEE Journal of Selected Topics in Signal Processing*, vol. 15, no. 6, 2021.
- [3] J. A. Zhang, M. L. Rahman, K. Wu, X. Huang, Y. J. Guo, S. Chen, and J. Yuan, "Enabling joint communication and radar sensing in mobile networks—A survey," *IEEE Communications Surveys Tutorials*, vol. 24, no. 1, pp. 306–345, 2022.
- [4] Z. Wang, Y. Liu, X. Mu, Z. Ding, and O. A. Dobre, "NOMA empowered integrated sensing and communication," *IEEE Commun. Lett.*, vol. 26, no. 3, pp. 677–681, 2022.
- [5] N. Zhao, Y. Wang, Z. Zhang, Q. Chang, and Y. Shen, "Joint transmit and receive beamforming design for integrated sensing and communication," *IEEE Commun. Lett.*, vol. 26, no. 3, pp. 662–666, 2022.
- [6] Z. Ni, J. A. Zhang, K. Yang, X. Huang, and T. A. Tsiftsis, "Multi-metric waveform optimization for multiple-input single-output joint communication and radar sensing," *IEEE Trans. Commun.*, vol. 70, no. 2, pp. 1276–1289, 2022.
- [7] F. Sohrabi, T. Jiang, W. Cui, and W. Yu, "Active sensing for communications by learning," *IEEE Journal on Selected Areas in Communications*, pp. 1–1, 2022.
- [8] L. Giroto de Oliveira, B. Nuss, M. B. Alabd, A. Diewald, M. Pauli, and T. Zwick, "Joint radar-communication systems: Modulation schemes and system design," *IEEE Trans. Microw. Theory Tech.*, vol. 70, no. 3, pp. 1521–1551, 2022.
- [9] Q. Shi, L. Liu, S. Zhang, and S. Cui, "Device-free sensing in OFDM cellular network," *IEEE Journal on Selected Areas in Communications*, pp. 1–1, 2022.
- [10] W. Wang, A. X. Liu, M. Shahzad, K. Ling, and S. Lu, "Device-free human activity recognition using commercial WiFi devices," *IEEE Journal on Selected Areas in Communications*, vol. 35, no. 5, pp. 1118–1131, 2017.
- [11] S. Sedighi, K. V. Mishra, M. R. B. Shankar, and B. Ottersten, "Localization with one-bit passive radars in narrowband internet-of-things using multivariate polynomial optimization," *IEEE Trans. Signal Process.*, vol. 69, pp. 2525–2540, 2021.
- [12] Y. Ma, B. Wang, W. Ning, and Y. Zhang, "PRSRTI: A novel device-free localization method using phase response shift based radio tomography imaging," *IEEE Transactions on Vehicular Technology*, vol. 69, no. 11, pp. 13 812–13 820, 2020.
- [13] Q. Wu and R. Zhang, "Intelligent reflecting surface enhanced wireless network via joint active and passive beamforming," *IEEE Trans. Wireless Commun.*, vol. 18, no. 11, pp. 5394–5409, 2019.
- [14] Q. Wu, Y. Zeng, and R. Zhang, "Joint trajectory and communication design for multi-UAV enabled wireless networks," *IEEE Trans. Wireless Commun.*, vol. 17, no. 3, pp. 2109–2121, 2018.
- [15] O. Rinchi, A. Elzanaty, and M.-S. Alouini, "Compressive near-field localization for multipath RIS-aided environments," *IEEE Commun. Lett.*, pp. 1–1, 2022.

[16] R. S. Prasobh Sankar, B. Deepak, and S. P. Chepuri, "Joint communication and radar sensing with reconfigurable intelligent surfaces," in *2021 IEEE 22nd International Workshop on Signal Processing Advances in Wireless Communications (SPAWC)*, 2021, pp. 471–475.

[17] R. Schmidt, "Multiple emitter location and signal parameter estimation," *IEEE Trans. Antennas Propag.*, vol. 34, no. 3, pp. 276–280, 1986.

[18] R. Roy and T. Kailath, "ESPRIT-Estimation of signal parameters via rotational invariance techniques," *IEEE Transactions on Acoustics, Speech, and Signal Processing*, vol. 37, no. 7, pp. 984–995, 1989.

[19] S. Sedighi, B. S. Mysore R, M. Soltanalian, and B. Ottersten, "On the performance of one-bit DoA estimation via sparse linear arrays," *IEEE Trans. Signal Process.*, vol. 69, pp. 6165–6182, 2021.

[20] P. Chen, Z. Cao, Z. Chen, and X. Wang, "Off-grid DOA estimation using sparse Bayesian learning in mimo radar with unknown mutual coupling," *IEEE Trans. Signal Process.*, vol. 67, no. 1, pp. 208–220, 2019.

[21] J. Dai and H. C. So, "Real-valued sparse Bayesian learning for DOA estimation with arbitrary linear arrays," *IEEE Transactions on Signal Processing*, vol. 69, pp. 4977–4990, 2021.

[22] Z. Wang, G. Sun, J. Tong, and Y. Ji, "Pattern synthesis for sparse linear arrays via atomic norm minimization," *IEEE Antennas Wireless Propag. Lett.*, vol. 20, no. 12, pp. 2215–2219, 2021.

[23] M. A. Abdelhay, N. O. Korany, and S. E. El-Khamy, "Synthesis of uniformly weighted sparse concentric ring arrays based on off-grid compressive sensing framework," *IEEE Antennas Wireless Propag. Lett.*, vol. 20, no. 4, pp. 448–452, 2021.

[24] Z. Wei, W. Wang, F. Dong, and Q. Liu, "Gridless one-bit direction-of-arrival estimation via atomic norm denoising," *IEEE Commun. Lett.*, vol. 24, no. 10, pp. 2177–2181, 2020.

[25] P. Chen, Z. Chen, Z. Cao, and X. Wang, "A new atomic norm for DOA estimation with gain-phase errors," *IEEE Trans. Signal Process.*, vol. 68, pp. 4293–4306, 2020.

[26] Z. Yang and L. Xie, "Enhancing sparsity and resolution via reweighted atomic norm minimization," *IEEE Trans. Signal Process.*, vol. 64, no. 4, pp. 995–1006, 2016.

[27] A. Govinda Raj and J. H. McClellan, "Single snapshot super-resolution DOA estimation for arbitrary array geometries," *IEEE Signal Process. Lett.*, vol. 26, no. 1, pp. 119–123, 2019.

[28] Y. Cui, J. Wang, H. Sun, H. Jiang, K. Yang, and J. Zhang, "Gridless underdetermined DOA estimation of wideband LFM signals with unknown amplitude distortion based on fractional Fourier transform," *IEEE Internet of Things Journal*, vol. 7, no. 12, pp. 11612–11625, 2020.

[29] M. Wagner, Y. Park, and P. Gerstoft, "Gridless DOA estimation and root-MUSIC for non-uniform linear arrays," *IEEE Trans. Signal Process.*, vol. 69, pp. 2144–2157, 2021.

[30] L. Zheng, M. Lops, and X. Wang, "Adaptive interference removal for uncoordinated radar/communication coexistence," *IEEE Journal of Selected Topics in Signal Processing*, vol. 12, no. 1, pp. 45–60, Feb. 2018.

[31] Y. Chi and M. F. D. Costa, "Harnessing sparsity over the continuum: Atomic norm minimization for superresolution," *IEEE Trans. Signal Process.*, p. 19, 2020.

[32] Y. Li and Y. Chi, "Off-the-grid line spectrum denoising and estimation with multiple measurement vectors," *IEEE Trans. Signal Process.*, vol. 64, no. 5, pp. 1257–1269, 2016.

[33] G. Tang, B. N. Bhaskar, P. Shah, and B. Recht, "Compressed sensing off the grid," *IEEE Trans. Inf. Theory*, vol. 59, no. 11, pp. 7465–7490, 2013.

[34] W. Liao and A. Fannjiang, "MUSIC for single-snapshot spectral estimation: Stability and super-resolution," *Applied and Computational Harmonic Analysis*, vol. 40, no. 1, pp. 33–67, 2016.

[35] M.-M. Zhao, Q. Wu, M.-J. Zhao, and R. Zhang, "Intelligent reflecting surface enhanced wireless networks: Two-timescale beamforming optimization," *IEEE Transactions on Wireless Communications*, vol. 20, no. 1, pp. 2–17, 2021.

[36] Z.-M. Liu, "Conditional Cramér–Rao lower bounds for DOA estimation and array calibration," *IEEE Signal Process. Lett.*, vol. 21, no. 3, pp. 361–364, 2014.

[37] B. Shi, N. Chen, X. Zhu, Y. Qian, Y. Zhang, F. Shu, and J. Wang, "Impact of low-resolution ADC on DOA estimation performance for massive MIMO receive array," *IEEE Systems Journal*, pp. 1–4, 2022.

[38] H. Chen, T. Ballal, and T. Y. Al-Naffouri, "DOA estimation with non-uniform linear arrays: A phase-difference projection approach," *IEEE Wireless Communications Letters*, vol. 10, no. 11, pp. 2435–2439, 2021.

[39] M. Lin, M. Xu, X. Wan, H. Liu, Z. Wu, J. Liu, B. Deng, D. Guan, and S. Zha, "Single sensor to estimate DOA with programmable metasur-

face," *IEEE Internet of Things Journal*, vol. 8, no. 12, pp. 10187–10197, 2021.

[40] X. Wei, D. Shen, and L. Dai, "Channel estimation for RIS assisted wireless communications—Part II: An improved solution based on double-structured sparsity," *IEEE Commun. Lett.*, vol. 25, no. 5, pp. 1403–1407, 2021.

[41] S. Ma, W. Shen, J. An, and L. Hanzo, "Wideband channel estimation for IRS-aided systems in the face of beam squint," *IEEE Trans. Wireless Commun.*, vol. 20, no. 10, pp. 6240–6253, 2021.

[42] I. W. Selesnick and I. Bayram, "Sparse signal estimation by maximally sparse convex optimization," *IEEE Trans. Signal Process.*, vol. 62, no. 5, pp. 1078–1092, 2014.

[43] Y. Li, Y. Sun, and Y. Chi, "Low-rank positive semidefinite matrix recovery from corrupted rank-one measurements," *IEEE Trans. Signal Process.*, vol. 65, no. 2, pp. 397–408, 2017.

APPENDIX A THE EXPRESSION OF FIM

The sub-matrices $\Omega_{1,1}$, $\Omega_{1,2}$, $\Omega_{1,3}$, $\Omega_{2,1}$, $\Omega_{2,2}$, $\Omega_{2,3}$, $\Omega_{3,1}$, $\Omega_{3,2}$, $\Omega_{3,3}$ in FIM are obtained as follows:

- $\Omega_{1,1}$ is obtained as

$$\begin{aligned} \Omega_{1,1} &= \mathcal{E} \left\{ \frac{\partial \ln^H f(\mathbf{r}(t); \zeta)}{\partial \boldsymbol{\theta}_{\text{TR}}} \frac{\partial \ln f(\mathbf{r}(t); \zeta)}{\partial \boldsymbol{\theta}_{\text{TR}}} \right\} \quad (55) \\ &= \mathcal{E} \left\{ \sigma_w^{-2} \{ \mathbf{B}^H \mathbf{G}^H [\mathbf{r}(t) - \boldsymbol{\mu}(t)] + \mathbf{B}^T \mathbf{G}^T \right. \\ &\quad \left. [\mathbf{r}(t) - \boldsymbol{\mu}(t)]^* \} \sigma_w^{-2} \{ [\mathbf{r}(t) - \boldsymbol{\mu}(t)]^H \mathbf{G} \mathbf{B} \right. \\ &\quad \left. + [\mathbf{r}(t) - \boldsymbol{\mu}(t)]^T \mathbf{G}^* \mathbf{B}^* \} \right\} \\ &= 2\sigma_w^{-2} \mathcal{R} \{ \mathbf{B}^H \mathbf{G}^H \mathbf{G} \mathbf{B} \}. \end{aligned}$$

- $\Omega_{2,2}$ is obtained as

$$\begin{aligned} \Omega_{2,2} &= \mathcal{E} \left\{ \frac{\partial \ln^H f(\mathbf{r}(t); \zeta)}{\partial \mathbf{z}(t)} \frac{\partial \ln f(\mathbf{r}(t); \zeta)}{\partial \mathbf{z}(t)} \right\} \quad (56) \\ &= \mathcal{E} \left\{ \sigma_w^{-2} \mathbf{A}^H(\boldsymbol{\theta}_{\text{TR}}) \mathbf{G}^H [\mathbf{r}(t) - \boldsymbol{\mu}(t)] \right. \\ &\quad \left. \sigma_w^{-2} [\mathbf{r}(t) - \boldsymbol{\mu}(t)]^H \mathbf{G} \mathbf{A}(\boldsymbol{\theta}_{\text{TR}}) \right\} \\ &= \sigma_w^{-2} \mathbf{A}^H(\boldsymbol{\theta}_{\text{TR}}) \mathbf{G}^H \mathbf{G} \mathbf{A}(\boldsymbol{\theta}_{\text{TR}}). \end{aligned}$$

- $\Omega_{3,3}$ is obtained as

$$\begin{aligned} \Omega_{3,3} &= \mathcal{E} \left\{ \frac{\partial \ln^H f(\mathbf{r}(t); \zeta)}{\partial q(t)} \frac{\partial \ln f(\mathbf{r}(t); \zeta)}{\partial q(t)} \right\} \quad (57) \\ &= \mathcal{E} \left\{ \sigma_w^{-2} \mathbf{a}^H(\boldsymbol{\theta}_{\text{AR}}) \mathbf{G}^H [\mathbf{r}(t) - \boldsymbol{\mu}(t)] \right. \\ &\quad \left. \sigma_w^{-2} [\mathbf{r}(t) - \boldsymbol{\mu}(t)]^H \mathbf{G} \mathbf{a}(\boldsymbol{\theta}_{\text{AR}}) \right\} \\ &= \sigma_w^{-2} \mathbf{a}^H(\boldsymbol{\theta}_{\text{AR}}) \mathbf{G}^H \mathbf{G} \mathbf{a}(\boldsymbol{\theta}_{\text{AR}}). \end{aligned}$$

- $\Omega_{1,2}$ is obtained as

$$\begin{aligned}\Omega_{1,2} &= \mathcal{E} \left\{ \frac{\partial \ln^H f(\mathbf{r}(t); \boldsymbol{\zeta})}{\partial \boldsymbol{\theta}_{\text{TR}}} \frac{\partial \ln f(\mathbf{r}(t); \boldsymbol{\zeta})}{\partial \mathbf{z}(t)} \right\} \quad (58) \\ &= \mathcal{E} \left\{ \sigma_w^{-2} \left\{ \mathbf{B}^H \mathbf{G}^H [\mathbf{r}(t) - \boldsymbol{\mu}(t)] + \mathbf{B}^T \mathbf{G}^T \right. \right. \\ &\quad \left. \left. [\mathbf{r}(t) - \boldsymbol{\mu}(t)]^* \right\} \sigma_w^{-2} [\mathbf{r}(t) - \boldsymbol{\mu}(t)]^H \mathbf{G} \mathbf{A}(\boldsymbol{\theta}_{\text{TR}}) \right\} \\ &= \sigma_w^{-2} \mathbf{B}^H \mathbf{G}^H \mathbf{G} \mathbf{A}(\boldsymbol{\theta}_{\text{TR}}).\end{aligned}$$

- $\Omega_{1,3}$ is obtained as

$$\begin{aligned}\Omega_{1,3} &= \mathcal{E} \left\{ \frac{\partial \ln^H f(\mathbf{r}(t); \boldsymbol{\zeta})}{\partial \boldsymbol{\theta}_{\text{TR}}} \frac{\partial \ln f(\mathbf{r}(t); \boldsymbol{\zeta})}{\partial q(t)} \right\} \quad (59) \\ &= \mathcal{E} \left\{ \sigma_w^{-2} \left\{ \mathbf{B}^H \mathbf{G}^H [\mathbf{r}(t) - \boldsymbol{\mu}(t)] + \mathbf{B}^T \mathbf{G}^T \right. \right. \\ &\quad \left. \left. [\mathbf{r}(t) - \boldsymbol{\mu}(t)]^* \right\} \sigma_w^{-2} [\mathbf{r}(t) - \boldsymbol{\mu}(t)]^H \mathbf{G} \mathbf{a}(\boldsymbol{\theta}_{\text{AR}}) \right\} \\ &= \sigma_w^{-2} \mathbf{B}^H \mathbf{G}^H \mathbf{G} \mathbf{a}(\boldsymbol{\theta}_{\text{AR}}).\end{aligned}$$

- $\Omega_{2,1}$ is obtained as

$$\begin{aligned}\Omega_{2,1} &= \mathcal{E} \left\{ \frac{\partial \ln^H f(\mathbf{r}(t); \boldsymbol{\zeta})}{\partial \boldsymbol{\theta}_{\text{TR}}} \frac{\partial \ln f(\mathbf{r}(t); \boldsymbol{\zeta})}{\partial q(t)} \right\} \quad (60) \\ &= \sigma_w^{-2} \mathbf{A}^H(\boldsymbol{\theta}_{\text{TR}}) \mathbf{G}^H \mathbf{G} \mathbf{B}.\end{aligned}$$

- $\Omega_{2,3}$ is obtained as

$$\begin{aligned}\Omega_{2,3} &= \mathcal{E} \left\{ \frac{\partial \ln^H f(\mathbf{r}(t); \boldsymbol{\zeta})}{\partial \mathbf{z}(t)} \frac{\partial \ln f(\mathbf{r}(t); \boldsymbol{\zeta})}{\partial q(t)} \right\} \quad (61) \\ &= \sigma_w^{-2} \mathbf{A}^H(\boldsymbol{\theta}_{\text{TR}}) \mathbf{G}^H \mathbf{G} \mathbf{a}(\boldsymbol{\theta}_{\text{AR}}).\end{aligned}$$

- $\Omega_{3,1}$ is obtained as

$$\begin{aligned}\Omega_{3,1} &= \mathcal{E} \left\{ \frac{\partial \ln^H f(\mathbf{r}(t); \boldsymbol{\zeta})}{\partial q(t)} \frac{\partial \ln f(\mathbf{r}(t); \boldsymbol{\zeta})}{\partial \boldsymbol{\theta}_{\text{TR}}} \right\} \quad (62) \\ &= \sigma_w^{-2} \mathbf{a}^H(\boldsymbol{\theta}_{\text{AR}}) \mathbf{G}^H \mathbf{G} \mathbf{B}.\end{aligned}$$

- $\Omega_{3,2}$ is obtained as

$$\begin{aligned}\Omega_{3,2} &= \mathcal{E} \left\{ \frac{\partial \ln^H f(\mathbf{r}(t); \boldsymbol{\zeta})}{\partial q(t)} \frac{\partial \ln f(\mathbf{r}(t); \boldsymbol{\zeta})}{\partial \mathbf{z}(t)} \right\} \quad (63) \\ &= \sigma_w^{-2} \mathbf{a}^H(\boldsymbol{\theta}_{\text{AR}}) \mathbf{G}^H \mathbf{G} \mathbf{A}(\boldsymbol{\theta}_{\text{TR}}).\end{aligned}$$